THE JOURNAL OF BIOLOGICAL CHEMISTRY VOL. 288, NO. 10, pp. 6777–6787, March 8, 2013

Zebrafish Collagen XIV Is Transiently Expressed in Epithelia and Is Required for Proper Function of Certain Basement Membranes*

Received for publication, October 24, 2012, and in revised form, January 10, 2013 Published, JBC Papers in Press, January 16, 2013, DOI 10.1074/jbc.M112.430637

Hannah L. Bader[‡§1] **Elise Lambert**[‡], **Alexandre Guiraud**[‡], **Marilyne Malbouyres**[‡], **Wolfgang Driever**[¶], **Manuel Koch**[§], **and Florence Ruggiero**[‡2]

From the [‡]*Institut de Génomique Fonctionnelle de Lyon, UMR 5242 CNRS, Ecole Normale Supérieure de Lyon, Université Lyon 1, F-69364 Lyon Cedex 07, France, the* [¶]*Department of Developmental Biology, Institute Biology 1, University of Freiburg, 79104 Freiburg, Germany, and the* [§]*Institute for Dental Research and Musculoskeletal Biology, Center for Biochemistry, Center for Molecular Medicine Cologne, Medical Faculty, University of Cologne, 50931 Cologne, Germany*

Background: Collagen XIV (COLXIV) is a component of connective tissues and regulates type I collagen fibril assembly in mice.
Results: Zebrafish COLXIV-A is transiently expressed in epithelia and incorporated into basement membranes (BMs).
Conclusion: COLXIV-A is a marker of epithelia in construction and is required for BM assembly.
Significance: We reveal COLXIV-A localization in embryonic epithelia and underlying BMs and its crucial role in proper BM formation.

We found that zebrafish has two differentially expressed *col14a1* paralogs. *col14a1a* expression peaked between 18-somite stage and 24 hours postfertilization (hpf), whereas *col14a1b* was first expressed at 32 hpf. To uncover functions of collagen XIV (COLXIV) during early embryogenesis, we focused our study on *col14a1a*. We characterized the α1 (XIV-A) chain as a collagenase-sensitive 200-kDa protein that formed dimer that could be reduced at high pH. As observed for the transcript, COLXIV-A protein expression peaked between 24 and 48 hpf. Using antisense probes and polyclonal antibodies, we show that *col14a1a* and its protein product COLXIV-A are transiently expressed in several epithelia, including epithelia undergoing shape changes, such as the fin folds. In contrast, anti-COLXII antibodies stained only connective tissues. COLXIV-A was also detected in the basement membrane (BM), where it co-localized with COLXII. At later developmental stages, COLXIV-A was not expressed in epithelia anymore but persisted in the BM. Morpholino knockdown of COLXIV-A provoked a skin detachment phenotype. Electron microscopy analysis revealed that morpholino-injected embryos lacked a lamina densa and lamina lucida at 24 hpf, and BM defects, such as gaps in the adepidermal granules, were still detected at 48 hpf. These BM defects were accompanied by a rupture of the dermis and detachment of the epidermis. Taken together, these data suggest an unexpected role of COLXIV-A in undifferentiated epithelia and in the formation of embryonic basement membranes.

Collagen XIV (COLXIV)[3] belongs to a subfamily of collagens called fibril associated collagens with interrupted triple helices (FACIT). COLXIV is a homotrimer with a trident-like structure (1). In the homotrimer, the trimerization of the collagenous domains forms a stem from which three long arms formed by the noncollagenous domains extend. COLXIV is found in many connective tissues, such as skin, tendon, and cornea (2–6). Electron microscopy studies have shown that COLXIV localizes *in vivo* to the surface of collagen I fibrils (4, 7, 8). In embryonic chick tendon, it is expressed when collagen fibrils elongate and ceases to be expressed when fibrils thicken (8), suggesting that COLXIV regulates collagen fibril assembly. Analysis of *Col14a1*-null mice further confirmed a role of COLXIV in early stages of collagen fibrillogenesis (9). However, COLXIV has been also shown to bind to a wide variety of cells (10–12), suggesting a possible role in cell function.

Here, we show that zebrafish COLXIV-A is transiently expressed in several undifferentiated epithelia and incorporated into the underlying BM. COLXIV is structurally closely related to COLXII, and these two collagens are often co-expressed (5, 6, 13). Using zebrafish anti-COLXII (14) and newly prepared anti-COLXIV-A antibodies, we found marked differences in the expression pattern of these two collagens: COLXII was expressed in connective tissues (14), whereas COLXIV-A was expressed in epithelia. However, their expression overlapped in the basement membrane and in particular in the epi-

* This work was supported by Agence Nationale de la Recherche Grant 10BLAN121901 and grants from the Emergence Research Program (Région Rhône-Alpes) and from the University Lyon 1 (Bonus Qualité Recherche).

[1] Recipient of a doctoral fellowship from the University Lyon1 and the German Academic Exchange Service. Present address: Boston University School of Medicine, Dept. of Medicine, Evans Biomedical Research Bldg. X-440, Boston, MA 022118.

[2] To whom correspondence should be addressed: Institut de Génomique Fonctionnelle de Lyon, ENS de Lyon, 46, allée d'Italie, F-69364 Lyon Cedex 07, France. Tel.: 33-426-731-358; Fax: 33-426-731-373; E-mail: florence.ruggiero@ens-lyon.fr.

[3] The abbreviations used are: COL, collagen; ECM, extracellular matrix; hpf, hours postfertilization; FACIT, fibril-associated collagens with interrupted triple helices; BM, basement membrane; MFF, median fin fold; FNIII, fibronectin type III; MO, morpholino; MS, mismatch control.

dermal-dermal basement membrane. Morpholino knockdown of COLXIV-A demonstrated a crucial role of this protein in the proper formation of the epidermal-dermal basement membrane and in the cohesion of the epidermis and the subjacent dermis. Our findings are in line with recent work showing that COLXII and COLXIV localize to anchoring plaques (*e.g.*, protein complexes involved in the attachment of the basement membrane to the skin) in human skin (13). Taken together, we demonstrate that 1) COLXIV-A is embryonically regulated, 2) collagens XII and XIV may have distinct spatiotemporal expression patterns during development, and 3) at early developmental stages, COLXIV-A has a role in undifferentiated epithelia and in the formation of the basement membrane.

EXPERIMENTAL PROCEDURES

Cloning of a Partial col14a1a cDNA—We have previously reported the cloning of a partial cDNA for zebrafish (AM941492) (14). This cDNA was used for the design of primers, *in situ* probes, and antibodies specific for *col14a1a* (see below). It should be noted that the sequence cloned by us is not identical to the hypothetical *col14a1a* mRNA sequence available in the NCBI database (XM_001922011; deduced from genomic sequence). XM_001922011 encodes a 5-amino acid insert missing in AM941492 (VSILG), and 7 amino acids differ in the two sequences. Furthermore, AM941492 encodes a 19-amino acid-long spacer (GWTTEFPTTIPTTTPI) separating the fifth and sixth fibronectin type III (FNIII) domain that is missing in XM_001922011. This discrepancy could not be simply explained by alternative splicing, because the sequence encoding this spacer was also not found in the genomic reference sequence database of NCBI. However, we believe that our cDNA (AM941492) is correct for the following reasons: 1) tetrapod COLXIV α1 chains have also a spacer between the fifth and the sixth FNIII domains; and 2) we obtained the same cDNA sequence with two independent RT-PCRs.

Recombinant Expression of FNIII Domains and Preparation and Characterization of Polyclonal Antibodies Specific for Zebrafish COLXIV-A—Polyclonal antibodies specific for zebrafish COLXIV-A were prepared as described previously (14). Briefly, clone AM941492 was subcloned into a bacterial expression vector, and the His-tagged fusion protein was affinity-purified with a nickel-Sepharose column. After removal of the His tag, the purified protein was used to immunize a rabbit and a guinea pig. The polyclonal antibodies obtained after sacrificing the animals were affinity-purified using a column of antigen coupled to Sepharose. To test the specificity of the affinity-purified antibodies, an ELISA assay was performed as described previously (14). Furthermore, the specificity of the antibodies was confirmed with a preincubation assay. Purified polyclonal guinea pig anti-zebrafish collagen XIV antibody diluted 1:250 in blocking solution was incubated with 8 μg of purified recombinant COLXIV-FNIII or 8 or 40 μg of COLXII-FNIII protein overnight at 4 °C. Subsequently, whole mount immunofluorescence staining of 48 hpf embryos was performed as described below. The immunofluorescence signal was efficiently extinguished by preincubation with COLXIV-FNIII domains but not COLXII-FNIII domains.

Fish Maintenance—Fish were maintained, and eggs were obtained essentially as previously described by Westerfield (15). Embryos were staged according to hours postfertilization (hpf) at 28.5 °C and according to morphological criteria (16). Different wild type strains (AB, AB/Tu, AB/TL, and fish from a pet shop) were used for expression pattern analysis. No differences in collagen expression between the different strains were observed.

Western Blot Analysis on Whole Embryos—Protein extracts from whole embryos at 24–120 hpf were prepared using Nonidet P-40 lysis buffer (1% (v/v) Nonidet P-40, 150 mM NaCl, 50 mM Hepes, pH 7.4, 5 mM EDTA, 10% (v/v) glycerol, and complete protease inhibitor mixture (Calbiochem)). After homogenization using a pellet pestle and centrifugation (13,000 $\times$ *g*, 15 min, 4 °C, protein concentration of supernatant was determined by BCA protein assay (Pierce), and equal amounts of proteins (20–25 μg) were loaded on SDS-polyacrylamide gel after heating for 5 min at 100 °C. For the study of the COLXIV-A electrophoretic pattern in SDS-PAGE, the electrophoresis sample buffer contained 90 mM Tris-HCl, pH 6.8, 8.0, 9.0, or 10.5 as indicated, 10% (v/v) glycerol, 5% (w/v) SDS, 0.02% (w/v) bromphenol blue.

Collagenase Digestion of the α1 Chain of Zebrafish Collagen XIV-A—Collagenase digestion was performed as described previously (14). Protein extracts from whole embryos at 24 hpf were prepared using Nonidet P-40 lysis buffer (1% (v/v) Nonidet P-40, 150 mM NaCl, 50 mM Hepes, pH 7.4, 5 mM EDTA, 10% (v/v) glycerol, and complete protease inhibitor mixture (Calbiochem)). After homogenization using a pellet pestle and centrifugation (13,000 $\times$ *g*, 15 min, 4 °C), protein concentration of the supernatant was determined, and 30 μg of proteins were incubated for 2 h at 4 or 37 °C with or without 200 units/ml collagenase (Worthington Biochemical Corporation) in enzymatic reaction buffer containing 5 mM $CaCl_2$ and 1 mM 4-(2-aminoethyl) benzenesulfonyl fluoride. The enzymatic reaction product was analyzed by Western blot using the affinity-purified polyclonal rabbit anti-zebrafish COLXIV-A antibodies (dilution 1:2000), followed by incubation with horseradish peroxidase-conjugated goat anti-rabbit IgG antibodies (Bio-Rad 170-6515; dilution 1:10,000) and revelation with a chemiluminescence substrate kit (Immun-Star WesternC chemiluminescent kit; Bio-Rad 170-5070).

RT-PCR—Total RNA was extracted from 20 embryos at various time points by using a Nucleospin® RNA II kit (Macherey-Nagel) according to the protocol for animal tissues. First strand cDNA synthesis was performed using Moloney murine leukemia virus reverse transcriptase (Promega), followed by amplification of desired cDNA by PCR with *Taq* DNA polymerase with ThermoPol buffer (BioLabs).

Whole Mount in Situ Hybridization—For the preparation of two different *col14a1a* specific probes, the partial cDNA AM941493 was digested with NcoI, and the resulting 686- and 406-bp fragments were subcloned and were used to prepare digoxigenin-labeled antisense probes (Roche Applied Science). Whole mount *in situ* hybridization was performed as previously described (17). 48- and 72-hpf embryos were pretreated with phenylthiourea to suppress pigmentation as described previously (14).

Whole Mount Immunofluorescence Staining—Whole mount immunofluorescence staining was performed as described previously (14). The following primary and secondary antibodies were used at the indicated dilutions: affinity-purified polyclonal guinea pig antibodies specific for zebrafish COLXIV-A, 1:250; affinity-purified rabbit polyclonal antibodies specific for zebrafish COLXIV-A, 1:500; affinity-purified rabbit polyclonal antibodies specific for zebrafish COLXII, 1:400 or 1:250; rabbit anti-laminin antibodies (Sigma L9393, chain specificity unknown), 1:200; anti-guinea pig IgG antibodies coupled to Cy2 or Cy3 (Jackson Immunoresearch), 1:200; anti-rabbit IgG coupled to Alexa488 (Invitrogen), 1:250; anti-guinea pig IgG coupled to Alexa 543 (Invitrogen), 1:250; and anti-rabbit IgG coupled to Alexa543 (Invitrogen), 1:400.

Morpholino Knockdown—Morpholinos (MO) and the mismatch control MS (MO sequence containing five base mismatches) were designed with sequences complementary to the *col14a1a* cDNA initial start codon region (Gene Tools): MO, 5′-CGACACCTGCATCCTTACAGCCAAG, and MS, 5′-CGAgACgTGCATaCTTAgAGCgAAG. One-cell stage embryos were injected with 4.2 ng of morpholinos diluted in sterile water. The morphological and phenotypic observations of morphants were performed with a stereomicroscope or a light microscope (all from Leica) equipped with a digital camera. MO-injected embryos were routinely compared with MS-injected, phenol red-injected, and noninjected embryos.

Histology and Transmission Electron Microscopy—Zebrafish embryos and larvae were processed as previously described (18). Whole embryos and larvae were sacrificed by incubation with excess of Tricaine and fixed overnight in 1.5% (v/v) glutaraldehyde and 1.5% (v/v) paraformaldehyde in 0.1 M cacodylate buffer (pH 7.4) at 4 °C followed by washing in 0.1 M cacodylate buffer, 10% (w/v) sucrose. The samples were then postfixed in 1% (v/v) osmium tetroxide for 1 h at room temperature, subsequently dehydrated in a graded series of ethanol, and embedded in epoxy resin. Thin sections were stained with methylene blue/azur II and observed with a light microscope (Leica) equipped with a digital camera (Nikon). Ultra thin sections were contrasted with uranyl acetate and lead citrate and observed with a Philips CM120 electron microscope, equipped with a digital CDD camera (Gatan), at the Centre Technique des Microstructures, University of Lyon 1.

Statistical Analysis—The results are given as the means ± S.E. The significance of differences between mean values was evaluated by Student *t* test (*, $p < 0.05$; **, $p < 0.01$; ***, $p < 0.001$).

RESULTS

Zebrafish Has Duplicate col14a1 Genes—In a search for zebrafish *col14a1*, we found two sequences with high homology to the chicken *col14a1* mRNA in the NCBI database: XM_001922011 and XM_003200499. These are mRNAs predicted on the basis of genomic sequences that are localized on chromosome 16 (XM_001922011) and chromosome 19 (XM_003200499), respectively. We will refer to these paralogs as *col14a1a* (XM_001922011) and *col14a1b* (XM_003200499). Both paralogs showed higher homology to tetrapod α1 (XIV) than to tetrapod α1 (XII) chains, confirming that they encode α1 (XIV) chains.

It should be noted that zebrafish has also two *col12a1* paralogs. We will refer to these as *col12a1a* (XM_002665259) and *col12a1b* (XM_686312). Our previously published *col12a1 in situ* probes are specific for *col12a1a* (14). Because the paralogs show high homology in the domains recognized by the antibodies (70% overall and 90% for the first fibronectin type III domain), our antibodies may recognize both paralogs. Because the specificity of the antibodies is unclear, we will refer simply to COLXII when describing data obtained with anti-COLXII antibodies.

Conserved Domain Organization of Zebrafish and Tetrapod α1 (XIV) Chains—Hypothetical protein sequences of the zebrafish α1 (XIV) chains are available in the NCBI database: XP_001922046, COLXIV-A; and XP_003200547, COLXIV-B. These protein sequences are deduced from genomic sequences. We used these sequences to analyze the domain organization of the zebrafish α1 (XIV) chains. For our analysis, we used the Scanprosite tool (ExPASy), combined with manual screening.

The N terminus of COLXIV-A consists of eight FNIII repeats alternating with two von Willebrand factor A domains and a thrombospondin N terminus-like domain. The C terminus consists of two short noncollagenous sequences (NC1 and NC2) and two collagenous domains (COL1 and COL2) (Fig. 1, *A* and *B*). This domain organization is identical to the domain organization of tetrapod COLXIV (19). In contrast, COLXIV-B is N-terminally truncated: it lacks the first von Willebrand factor A domain and the first three FNIII domains (Fig. 1*A*). However, it is very likely that the *col14a1b* sequence is still incomplete, because it lacks an N-terminal signal peptide, which is a feature of all secreted ECM proteins, including tetrapod COLXIV and zebrafish COLXIV-A. Unfortunately, we were so far unable to find the missing sequence in databases.

Both zebrafish α1 (XIV) chains have the typical FACIT signature, *e.g.*, two short collagenous domains alternating with two noncollagenous domains at the C terminus. Furthermore, as is the case in all FACITs, the COL1 domain has two imperfections: two interruptions in the G*XX* triplet repeats and a conserved C*XXXX*C motif found at the NC1-COL1 junction (Fig. 1, *B* and *C*). In addition, as described for tetrapod COLXII and COLXIV, the COL2 domain has also an imperfection (Fig. 1*B*). The triple-helical imperfections and the cysteine motif are highly conserved between paralogs and between species (Fig. 1, *B* and *C*).

col14a1a and col14a1b Are Differentially Expressed during Embryogenesis—Semi-quantitative RT-PCR showed that *col14a1a* and *col14a1b* are differentially expressed; *col14a1a* was first detected at 18 hpf and peaked between 18 and 24 hpf (Fig. 2*A*). In contrast, *col14a1b* mRNA expression started later (32 hpf) and continued to be expressed at high levels at late developmental stages (48–120 hpf). The *col12a1* paralogs also showed a differential expression pattern. *col12a1a* was detected at all developmental stages analyzed, including very early embryogenesis (2.5 hpf), indicating that it is a maternal transcript, whereas *col12a1b* was first detected at 18 hpf (Fig. 2*A*).

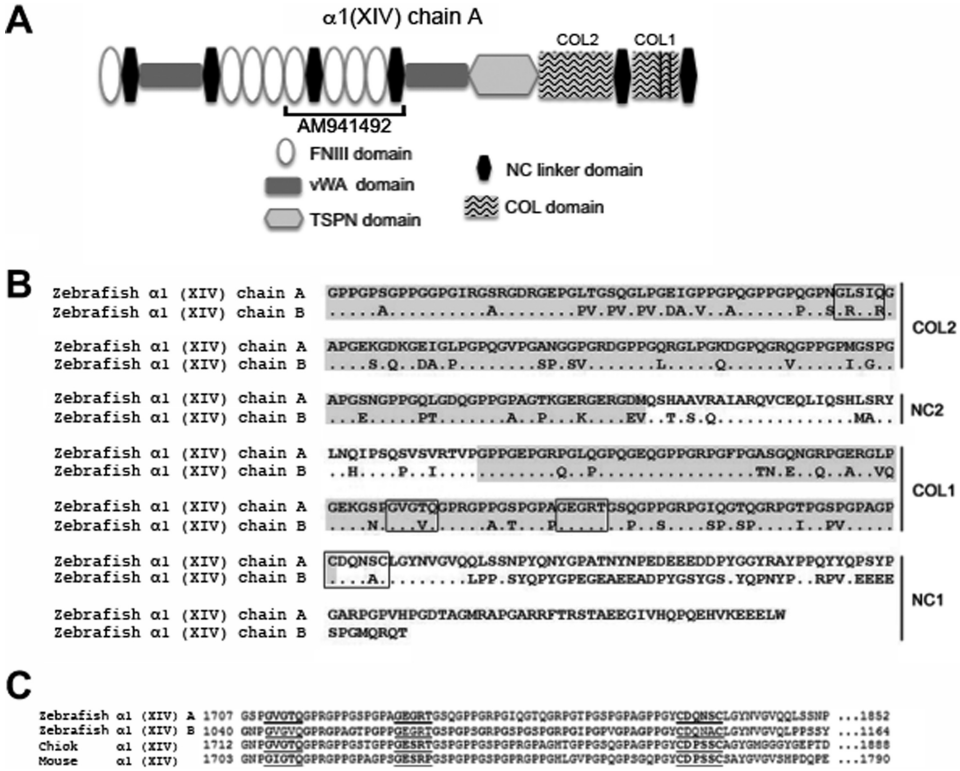

FIGURE 1. **Structure of the zebrafish collagen α1(XIV-A) and α1(XIV-B) chains.** *A*, schematic representation of the structure of the tetrapod collagen α1(XIV) chain. The domain organization is conserved in the zebrafish *col14a1a* ortholog. The *col14a1b* sequence is still incomplete and lacks currently the first von Willebrand factor A domain and the first three FNIII domains. The partial cDNA AM941492, which encompasses the FNIII domains 5–8 of the zebrafish α1 (XIV-A) chain, was used for the preparation of PCR primers, antisense probes, and polyclonal antibodies. *COL1*, collagenous domain 1; *COL2*, collagenous domain 2; *NC*, noncollagenous domains; *TSPN*, thrombospondin N-terminal like domain; *vWA*, von Willebrand factor A domain; *FNIII*, fibronectin type III domain. The *vertical lines* indicate interruptions of the triple helix in the COL1 domain. *B* and *C*, C terminus of the zebrafish α1(XIV-A) and α1(XIV-B) chains showing that both paralogs exhibit the features of a FACIT collagen. *B*, amino acid sequence of the C termini of the zebrafish α1(XIV-A) and α1(XIV-B) chains (XP_001922046, NCBI, COLXIV-A; and XP_003200547, NCBI, COLXIV-B); collagenous domains 1 and 2 are *shaded*, and imperfections of the triple helix, as well as the conserved C*XXXX*C motif at the NC1-COL1 junction, are *boxed*. *C*, amino acid sequence alignment of the C termini of the zebrafish (XP_001922046, NCBI, COLXIV-A; and XP_003200547, NCBI, COLXIV-B), chicken (Swiss-Prot P32018), and mouse (Swiss-Prot Q80X19) COLXIV α1 chain at the C*XXXX*C motif. The conserved C*XXXX*C motif at the NC1-COL1 junction and the two conserved imperfections in the first collagenous domain are *underlined*.

In other species, *col14a1* expression has been mainly analyzed at late developmental stages. The fact that *col14a1a* expression peaked at early developmental stages (18 to 24 hpf) suggested that an analysis of its expression pattern might uncover previously unreported functions of *col14a1* in early embryogenesis. Also, *col14a1a* showed higher homology to chicken *col14a1* than *col14a1b* (60% identity, 73% conserved *versus* 48% identity, 60% conserved on the protein level). Finally, human *COL14A1* gene has been previously mapped to chromosome 8q23 (20). Using Ensembl for *in silico* chromosome mapping analysis, we demonstrate that the orthologous gene triplet *DEPTOR*/*COL14A1*/*MRPL13* observed in the *Homo sapiens* genome is conserved (*deptor*/*col14a1a*/*mrpl13*) in chromosome 16 of the *Danio rerio* genome. No conserved synteny was observed in the chromosomal region containing *col14a1b*. For all these reasons, we decided to focus our subsequent expression pattern analysis on *col14a1a.*

col14a1a Expression Is Developmentally Regulated—In situ hybridization confirmed the absence of *col14a1a* expression before somitogenesis (data not shown) as previously reported (21) with cb542 probe. At the 18-somite stage, *col14a1a* transcripts were detected in neural and epidermal/peridermal tissues. Neurectodermal structures include telencephalic regions, the ear placode, and a narrow band within the brain (Fig. 2*B*, *panel b*, *arrow*) that likely corresponds to the midbrain-hindbrain boundary because signal was clearly detected in the midbrain-hindbrain boundary at 24 hpf (Fig. 2*B*, *panel d*). Ectodermal structures include parts of the epidermis (Fig. 2*B*, *panels a* and *b*) and the nascent fin fold (Fig. 2*B*, *panel c*). At 24 hpf, expression in the telencephalon and the ear placode is strongly reduced, and expression appeared in the nasal placode, the midbrain-hindbrain boundary and in pharyngeal pouches 2 and 3. A small *col14a1a*-positive area was observed in the roof of the forebrain, which corresponds to the pineal organ location (Fig. 2*B*, *panel d*, *arrowhead*). Furthermore, *col14a1a* expression persisted throughout the skin and the developing fin fold (Fig. 2*B*, *panels e* and *f*). At 48 hpf, *col14a1a* expression in the skin could not be distinguished from background staining (Fig. 2*B*, *panel h*). In the head, expression was restricted to the otic anterior macula and the pharyngeal arch endoderm (Fig. 2*B*, *panels g* and *h*). In addition, a strong signal was observed in the apical fin fold of the pectoral fin bud (Fig. 2*B*, *panel i*). At 72 hpf, *col14a1* mRNA was detected in the gut (Fig. 2*B*, *panel j*), and expression persisted in the anterior macula (Fig. 2*B*, *panel k*), whereas expression in the fin fold had ceased (data not shown), and only a very weak signal was detected in the apical fin fold of the pectoral fin bud (Fig. 2*B*, *panel l*).

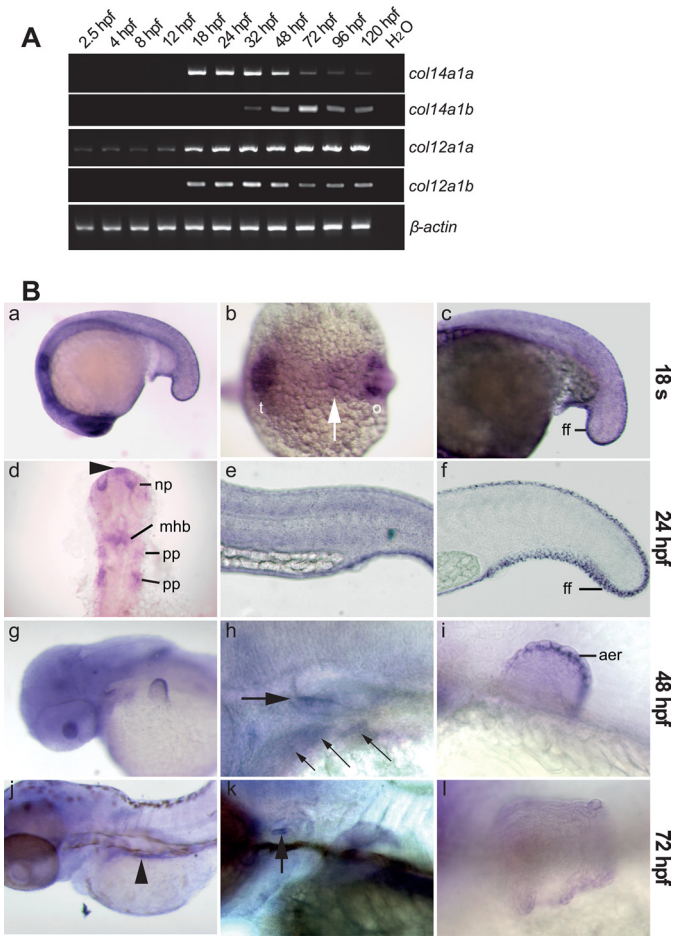

FIGURE 2. **Temporal and spatial expression patterns of the zebrafish *col14a1a* gene.** *A*, expression profiles of the closely related *col14a1a*, *col14a1b*, *col12a1a*, and *col12a1b* genes analyzed by RT-PCR of mRNA extracts from wild type embryos at the indicated developmental time points. *β-actin* was used as housekeeping gene internal control. *B*, whole mount *in situ* hybridization with *col14a1a* specific antisense probes of embryos at 18-somite stage (*panels a–c*), 24 hpf (*panels d–f*), 48 hpf (*panels g–i*), and 72 hpf (*panels j–l*). *Panels a*, *c*, *e*, *f*, *h*, *i*, *k*, and *l*, lateral view (dorsal is *up*, and anterior is to the *left*). *Panel b*, dorsal view, anterior left. *Panel d*, flat mount (anterior is *up*). *Panels g* and *j*, dorso-lateral view (anterior to the *left*, and dorsal is *up*). The embryos shown in *panels d* and *f* were developed shorter than the embryo shown in *panel e* to reveal the staining in the head and the fin fold, which is otherwise obscured by the strong signal in the skin. At the 18-somite stage (*panels a–c*), the *col14a1a* specific probe stains the skin throughout the embryo and within the head (*panel a*), a band (*arrow*) between the telencephalon and the otic placode (*panel b*), and the nascent median fin fold (*panel c*). At 24 hpf (*panels d–f*), *col14a1a* mRNA is detected in the roof of the forebrain (*arrowhead*, *panel d*), the olfactory placode/nasal pit, the midbrain-hindbrain boundary, and the pharyngeal pouches; expression in the skin (*panel e*) and in the median fin fold (*panel f*) is maintained. *Panels g–i*, at 48 hpf, *col14a1a* mRNA is detected in the gill endoderm (*panel h*, *small arrows*) and the otic anterior macula (*panel h*, *thick arrow*), within the pectoral fin bud (*panel g* and *i*), in the apical fin fold/apical ectodermal ridge (detail, *panel i*). *Panels j–l*, at 72 hpf, *col14a1a* is strongly expressed in the gut (*panel j*, *arrowhead*) and in the anterior macula (*panel k*, *arrow*), whereas expression within the pectoral fin bud has ceased (*panel l*). *t*, telencephalon; *ff*, fin fold; *o*, otic placode; *mhb*, midbrain-hindbrain boundary; *pp*, pharyngeal pouches; *aer*, apical ectodermal ridge; *np*, olfactory placode/nasal pit.

Characterization of Zebrafish COLXIV-A Protein—We prepared polyclonal antibodies against zebrafish COLXIV-A and used them to characterize the zebrafish α1 (XIV-A) chain. In a Western blot with protein extracts from 24-hpf zebrafish embryos, a band of ~200 kDa was detected, corresponding to the expected molecular weight of COLXIV-A. Furthermore, this band was, as expected, collagenase-sensitive. COLXIV-A consists predominantly of noncollagenous domains, and collagenase treatment results therefore only in a small shift of the band when analyzed by SDS-PAGE (Fig. 3*A*). Interestingly, COLXIV-A is perfectly soluble in the Nonidet P-40 lysis buffer because no protein was detected in the insoluble fraction by Western blot (data not shown).

A second band (significantly above 200 kDa) was also detected in addition to the ~200-kDa band (Fig. 3*A*). Such an electrophoretic pattern has been previously described for both tetrapod COLXII and COLXIV, and it was found that the upper band corresponds to a disulfide bonded dimer of the α1 chain that is resistant to β-mercaptoethanol-mediated reduction in standard conditions (22, 23). Here, we show that alkalinization of the sample buffer from pH 6.8 to 8 resulted in a decrease of the upper band intensity with a concomitant increase of the ~200-kDa band intensity (Fig. 3*B*). This strongly suggests that the upper band corresponds to a dimer of zebrafish α1(XIV) chains. A further increase in pH to pH 9 and 10.5 allowed complete dissociation of dimer into monomer as assessed by the disappearance of the upper band. These results show that COLXIV resolution by SDS-PAGE reveals a ~200-kDa band corresponding to monomer of α1(XIV) chain and an upper band corresponding to dimer whose dissociation by β-mercaptoethanol is pH-sensitive. It should be noted that the bands recognized by anti-COLXIV-A antibodies were efficiently extinguished by morpholinos directed against COLXIV-A, confirming the specificity of the antibodies and excluding the possibility of cross-reaction with COLXIV-B (see Fig. 7*A*).

COLXIV-A Protein Expression Peaks between 24 and 48 hpf—Protein expression was analyzed on total protein extracts of 24–120-hpf embryos (Fig. 3, *C* and *D*). It should be noted that it did not make a difference whether deyolked or undeyolked embryos were used for the protein expression analysis. Because the various loading controls commonly used in the literature (GAPDH, β-actin, tubulin, or acetylated tubulin) varied significantly during the early stages of development (between 24 and 48 hpf), we quantified the protein expression of both collagens by comparing them with acetylated tubulin protein amounts (Fig. 3*D*), as well as β-actin expression (data not shown). Similar results were observed with both control proteins. We thus demonstrate that COLXIV-A is highly expressed very early during zebrafish development (at 24 and 48 hpf), and this strong expression drastically and significantly decreases from 72 hpf until 120 hpf. In contrast, COLXII protein expression continuously increased from 24 to 120 hpf.

COLXIV-A Is Detected in Undifferentiated Epithelia and Subjacent BMs—Immunofluorescence staining of whole embryos was then performed to determine the location of COLXIV-A during embryonic development. At 24 hpf, COLXIV-A was expressed in several epithelia (Fig. 4). In agreement with the *in situ* hybridization data, COLXIV-A was detected in three cranial placodes, *e.g.*, the nasal/olfactory placode, the lens, and the ear/otic placode (Fig. 4*A*). COLXIV-A was also detected in the BM encasing the placodes and in the meninges (Fig. 4, *A* and *B*). Interestingly, however, COLXIV-A was expressed not only in basal placodal cells, which synthesize the BM components, but also throughout the entire placodal

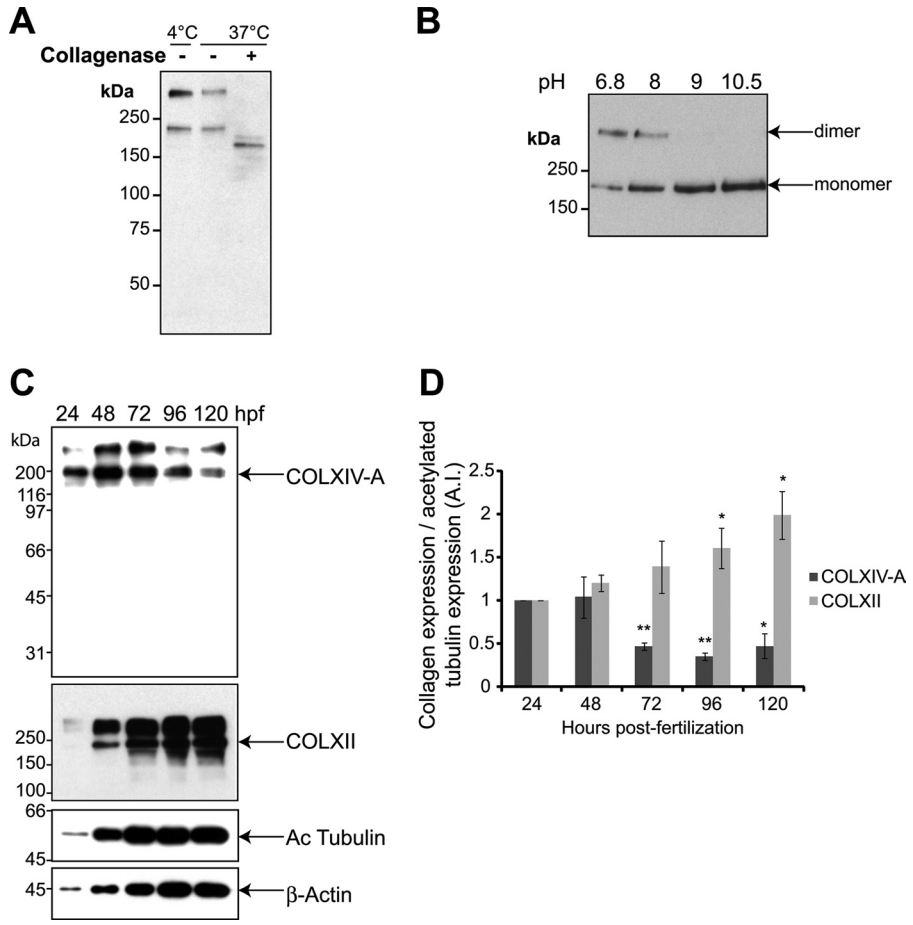

FIGURE 3. **Characterization of the collagen α1(XIV-A) chain and expression profile of the COLXIV-A protein.** *A*, protein extracts from 24-hpf whole zebrafish embryos were treated with (+) or without (−) collagenase at 4 or 37 °C. Western blot was performed with affinity-purified polyclonal rabbit anti-zebrafish collagen XIV-A antibodies. *B*, dimer reduction analysis. 72-hpf embryo protein extracts were boiled for 3 min in electrophoresis sample buffer supplemented with β-mercaptoethanol in Tris-HCl buffer at various pH. SDS-PAGE was performed using a 5% acrylamide separating gel. *C*, whole cell extracts of 24–120-hpf wild type embryos were analyzed by Western blot using anti-zebrafish collagen XIV-A, anti-zebrafish collagen XII, anti-β-actin, and anti-acetylated tubulin antibodies. Note that the *upper band* seen with anti-COLXII antibodies corresponds to a dimer that is resistant to β-mercaptoethanol-mediated reduction under standard conditions, as described for COLXIV-A (see text). The blot shown is representative of three separate experiments. *D*, quantification of collagen XIV-A and XII expression compared with acetylated tubulin expression. The results are expressed as an index corresponding to the collagen expression at 24 hpf compared with the other time points (collagen expression/acetylated tubulin expression at 24 hpf; index = 1) and correspond to the means ± S.E. of three separate experiments.

tissue (Fig. 4*A*). The placodes originate from the ectoderm and still retain at 24 hpf characteristics of the surface epithelium (24–27). This epithelial expression pattern contrasted strikingly with the expression pattern of COLXII, which was detected in the connective tissue surrounding the placodes (Fig. 4*B* and Ref. 14). However, COLXII and COLXIV-A staining coincided in the basement membrane (Fig. 4*B*). This is in agreement with our previous work that showed that COLXII is present in the immediate vicinity of the basement membrane (the basement membrane zone, a junctional zone with protein complexes that link the BM to the subjacent connective tissue) (14).

At 24 hpf, COLXIV-A was also detected in basal epidermal cells, and the epidermal-dermal BM (Fig. 4*C*). Interestingly, within the basal epidermal cells, COLXIV-A did not show a polarized distribution but could be detected both at the apical and basal poles (Fig. 4*C*).

In addition to these ectodermal derived epithelia, COLXIV-A was also detected in epithelia of endodermal origin. At 24 hpf, COLXIV-A was detected in the second and third pharyngeal pouch (identified by the marker Zn8; Fig. 4*D*), and at 72 hpf, it was detected in the gut (Fig. 4*E*).

COLXIV-A Expression Ceases in Differentiated Epithelia but Persists in BMs—At 48 and 72 hpf, when the differentiation of organs and tissues is well advanced in zebrafish, COLXIV-A was not detected in epithelia anymore. Because the expression pattern of COLXIV-A was essentially the same at 48 and 72 hpf, we will describe here only the expression pattern at 72 hpf. At 72 hpf, COLXIV-A could not be detected anymore in the olfactory placode (Fig. 5*A*), the lens (Fig. 5*B*), basal epidermal cells (Fig. 5*C*), and the gill endoderm (Fig. 5*D*).

In the otic placode, COLXIV-A became restricted to the anterior macula, which is one of three sensory patches involved in the detection of rotation and acceleration in teleost. Interestingly, COLXIV-A was detected within the sensory neurons of the macula (Fig. 5*E*). The only other epithelium in which COLXIV-A was detected at 72 hpf was the gut (Fig. 4*E*). However, the gut is the last organ to form, and at 72 hpf, the gut epithelium has not yet started to differentiate (28), corroborating that COLXIV-A is specifically expressed in undifferentiated epithelia.

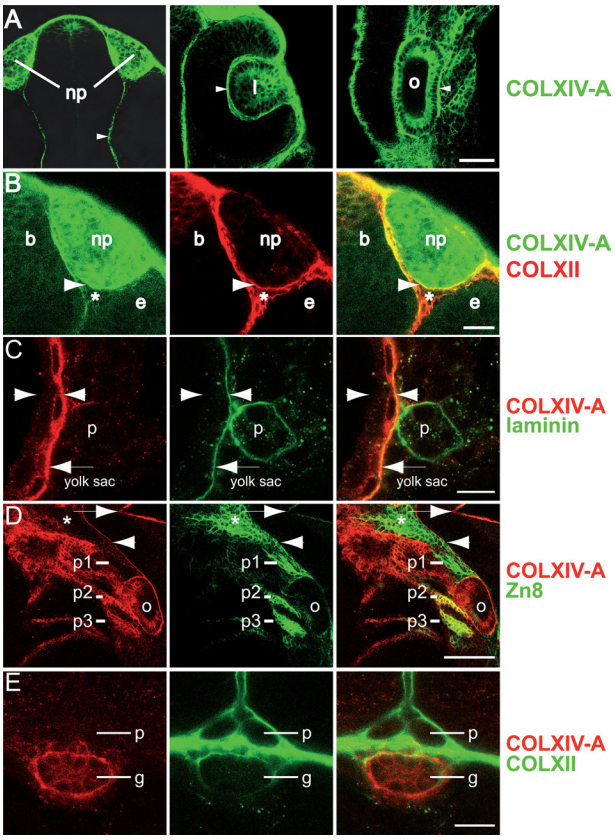

FIGURE 4. **Collagen XIV-A is expressed in cranial placodes, ectodermal and endodermal epithelia and subjacent BMs.** Shown are whole mount immunofluorescence stainings of 24- and 72-hpf embryos stained with antibodies as indicated and analyzed with confocal microscopy. *Row A*, at 24 hpf, COLXIV-A is detected in cranial placodes: the olfactory placode/nasal pit (*np*), the lens (*l*), and the otic placode (*o*). COLXIV-A is also detected in the meninges (*arrowhead*, *left panel*) and the BM encasing the lens and the otic placode (*arrowheads*, *middle* and *right panels*, respectively). Shown is a flat mount of the head (anterior is *up*). *Row B*, at 24 hpf, collagens XII and XIV-A are expressed in connective tissues and epithelia, respectively. COLXIV-A is expressed within the nasal pit (*np*), whereas COLXII is expressed in the surrounding connective tissue (see *asterisk*), including the connective tissue between brain (*b*), nasal pit (*np*), and eye (*e*). COLXIV-A staining overlaps with COLXII staining in the BM encasing the nasal pit (*arrowhead*). The *left* and *middle panels* show single stainings, and the *right panel* shows merged images. *Row C*, at 24 hpf, COLXIV-A is expressed in basal epidermal cells and the subepidermal BM. A transversal section of the tail at the level of the yolk sac extension is shown, zooming in on the region surrounding the pronephric duct (*p*). *Arrowheads* indicate the borders of the epidermis. The *arrow* points to the subepidermal BM, where COLXIV-A staining coincides with laminin staining. The *left* and *middle panels* show single stainings, and the *right panel* shows merged images. *Row D*, at 24 hpf, COLXIV-A is expressed in pharyngeal pouches 2 and 3. A lateral view of the head is shown, zooming in on pharyngeal pouches 1–3 (*p1–p3*); the arrow indicates the posterior edge of midbrain-hindbrain boundary, and the *arrowhead* indicates the meninges. The *asterisk* indicates the anterior part of pharyngeal pouch 1. Note that COLXIV-A staining coincides with the pharyngeal pouch marker Zn8 in pouches 2 and 3. The *left* and *middle panels* show single stains, and the *right panel* shows merged images. *Row E*, at 72 hpf, COLXIV-A is detected within the epithelium of the gut (*g*) but not the pronephric ducts (*p*). A transveral section at the level of the yolk sac extension is shown. The *left* and *middle panels* show single stains, and the *right panel* shows merged images. *Scale bars*: *row C*, 10 μm; *row D*, 50 μm; *row E*, 20 μm. For simplicity, colors of COL XIV and Zn8 stainings were reversed in *row D* to match *rows C* and *E*.

COLXIV-A Is Expressed in the Median and Apical Fin Fold—The median fin fold (MFF) and the apical fold of the pectoral fin bud are epithelial folds with a core of connective tissue. It is thought that the outgrowth of the fin folds involves cell shape changes of a tip cell, as well as proliferation (29, 30). In agree-

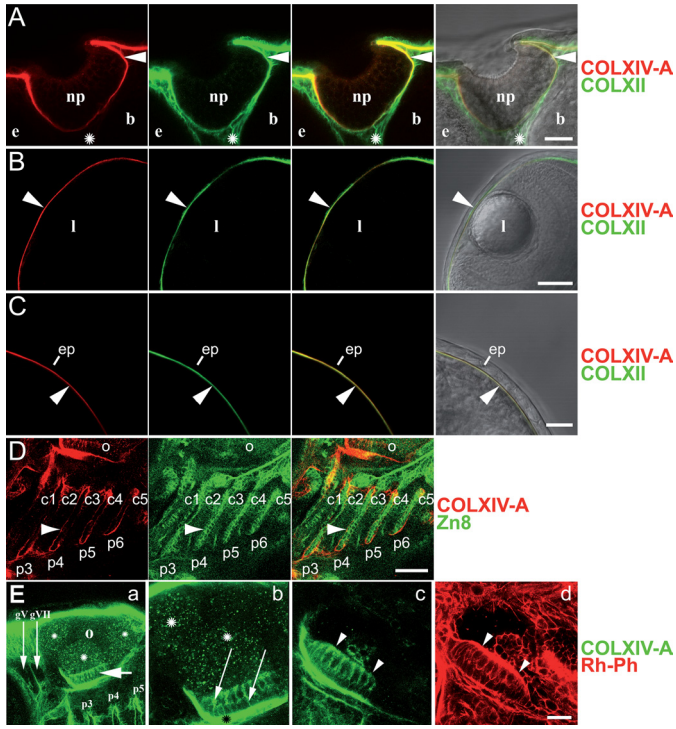

FIGURE 5. **Collagen XIV-A ceases to be expressed in differentiated epithelia but can still be detected in subjacent BMs.** Shown are whole mount immunofluorescence stainings of 72-hpf embryos stained with the indicated antibodies; all of the images are confocal microscope images. *Row A*, at 72 hpf, COLXIV-A is not expressed within the olfactory placode/nasal pit (*np*) anymore but can be still detected in the subjacent BM (*arrowhead*), where it co-localizes with COLXII. COLXII, but not COLXIV-A, is detected in the connective tissue (labeled with an *asterisk*) between nasal pit (*np*), brain (*b*), and eye (*e*). A dorsal view of the head is shown (anterior is *up*, and median is to the *right*). Shown are, from *left* to *right*, COLXIV-A staining (*red*), COLXII staining (*green*), an overlay of both stainings, and an overlay of COL XIV-A and COLXII stainings with the bright field image. *Row B*, at 72 hpf, COLXIV-A is not expressed in the lens (*l*) anymore but can be detected in the corneal BM (*arrowhead*), where it co-localizes with COLXII. A dorsal view of the head is shown (anterior is *up*, and median is to the *right*). Shown are, from *left* to *right*, COLXIV-A staining (*red*), COLXII staining (*green*), an overlay of both stainings, and an overlay of COL XIV-A and COLXII stainings with the bright field image. *Row C*, at 72 hpf, COLXIV-A is not expressed in the epidermis (*ep*) anymore but can be still detected in the subjacent BM (*arrowhead*). A dorsal view of the head is shown (anterior is *up*, and median is to the *left*). Shown are, from *left* to *right*, COLXIV-A staining (*red*), COLXII staining (*green*), an overlay of both stainings, and an overlay of COLXIV-A and COLXII stainings with the bright field image. *Row D*, at 72 hpf COLXIV-A is not expressed within the pharyngeal pouches anymore (labeled with the marker Zn8) but is now detected in the BM subjacent to the pharyngeal pouch epithelium (*arrowhead*). *c1–c5*, ceratohyals of gill-bearing pharyngeal arches 3–7; *p3–p6*, pharyngeal pouches 3–6; *o*, otic placode. A lateral view of the head is shown (anterior is to the *left*). Shown are, from *left* to *right*, COLXIV-A staining (*red*), Zn8 staining (*green*), and an overlay of both stainings. *Row E*, collagen XIV-A is expressed in the otic anterior macula. A lateral view of the head is shown (anterior is to the *left*, and dorsal is *up*). *Row E*, *panel a*, COLXIV is expressed in the anterior macula (*short arrow*) and is also detected in the epineuria of the cranial ganglia V (*gV*) and VII (*gVII*) (*long arrows*). *p3–p5*, pharyngeal pouches 3–5. *Asterisks* indicate unspecific staining of the lumen of the otic placode (*o*). *Row E*, *panel b*, higher magnification of the anterior macula showing that anti-COLXIV-A antibodies stain both the apical, sensory cell layer and the basal, support cell layer of the macula (see *arrows*). Staining is also observed in the subjacent ECM (*black asterisk*). *White asterisk*, unspecific staining of the lumen. *Panels c* and *d*, fluorescence staining with antibodies specific for COLXIV-A (*panel c*, *green*) and fluorochrome (rhodamin) coupled phalloidin (*Rh-Ph*, *panel d*, *red*); phalloidin binds to F-actin and labels the hairs of hair cells (*arrowheads*); COLXIV-A is absent from the ECM covering the hairs. *Scale bars*: rows *A*, *C*, and *E*, *panels b–d*, 20 μm; *rows B* and *D*, 50 μm; *row E*, *panel a*, 40 μm.

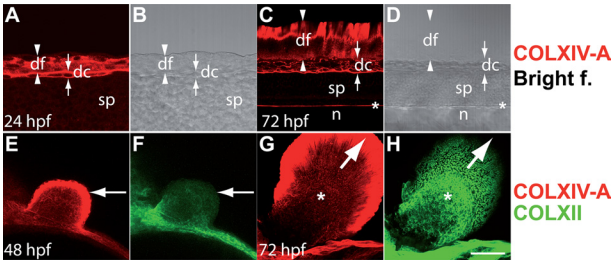

FIGURE 6. **COLXIV-A is expressed in the median fin fold and the apical fold of the pectoral fin bud.** Whole mount immunofluorescence staining is shown; all of the images are confocal images. *A–D*, lateral view of the tail at 24 hpf (*A* and *B*) and 72 hpf (*C* and *D*), respectively. *A–D* show median optical sections (anterior is to the *left*, and dorsal is *up*). *A–D*, immunofluorescence staining with antibodies specific for COLXIV-A (*red*). COLXIV-A staining (*A*) and the bright field image (*B*) are shown. COLXIV-A is expressed throughout the dorsal fin fold (*df*) and in the dorsal connective tissue subjacent to the fin fold (*dc*). *C* and *D*, COLXIV-A staining (*C*) and the bright field image (*D*) are shown. *C* and *D*, dorsal fin fold (*df*) at 72 hpf. At this stage, COLXIV-A antibodies stain only the distal rim of the median fin fold. COLXIV-A continues to be expressed in the dorsal connective tissue (*dc*) and is also detected in the meninges (*asterisk*). The *arrowheads* and *arrows* indicate the borders of the dorsal fin fold (*df*) and the dorsal connective tissue (*dc*), respectively. *sp*, spinal cord; *n*, notochord. *E–H*, pectoral fin buds of embryos at 48 hpf (*E* and *F*) and 72 hpf (*G* and *H*) co-stained with antibodies specific for COLXIV-A (*red*) and COLXII (*green*). At 48 hpf, COLXIV-A is detected throughout apical fold of the pectoral fin bud (*arrow*), whereas COLXII is not yet expressed in the fin bud. *G* and *H*, at 72 hpf, COLXIV-A is restricted to the distal rim of the apical fold (*arrow*), and COLXII is now expressed in the fin bud mesenchyme (*asterisk*). *Scale bars*: *A* and *B*, 25 μm; *C–H*, 50 μm.

ment with the *in situ* data (Fig. 2*B*, *panel f*), COLXIV-A protein was detected at 24 hpf in the nascent median fin fold (Fig. 6, *A* and *B*). The fin fold epithelium is an extension of the epidermis. As described above, COLXIV-A is only expressed in basal epidermal cells (Fig. 4*C*). COLXIV-A was also restricted to the basal epidermal layer in the MFF (Fig. 6, *A* and *C*; the distal rim of the fin fold is not stained). At 72 hpf, COLXIV-A co-localized with laminin in the distal fin fold (Fig. 6, *C* and *D*, and data not shown). At this stage, the fin fold is pointed: it has proximally a thick base and tapers off, becoming very thin distally. In a median optical section of the MFF, the connective tissue core is therefore visible proximally, and the BM is visible distally. COLXIV-A was at this stage not detected in the proximal fin fold, indicating that it was not expressed in the connective tissue core (Fig. 6, *C* and *D*). It was also not detected in the fin fold epithelium anymore (data not shown). In contrast, COLXII was not detected in the MFF at 24 hpf and localized to the connective tissue core at 72 hpf (data not shown and Ref. 14). Both collagens could be detected in the connective tissue beneath the MFF (Fig. 6, *C* and *D*, and Ref. 14). A similar staining pattern was observed in the apical fin fold of the pectoral bud, *e.g.*, COLXIV-A was expressed in the epithelium of the nascent apical fold at 48 hpf but was restricted to the BM at 72 hpf (Fig. 6, *E* and *G*). In contrast, COLXII was not expressed in the apical fin fold at 48 hpf, and could be detected only within the connective tissue of the apical fin fold at 72 hpf (Fig. 6, *F* and *H*). Taken together, the expression pattern of COLXIV-A suggests that it is involved in the morphogenesis and outgrowth of the median and apical fin fold.

COLXIV-A Knockdown Results in Defects in BM Structure and Impaired Dermal Cohesion—To analyze the function of COLXIV-A, we performed morpholino knockdown of COLXIV-A in developing embryos. One-cell stage embryos

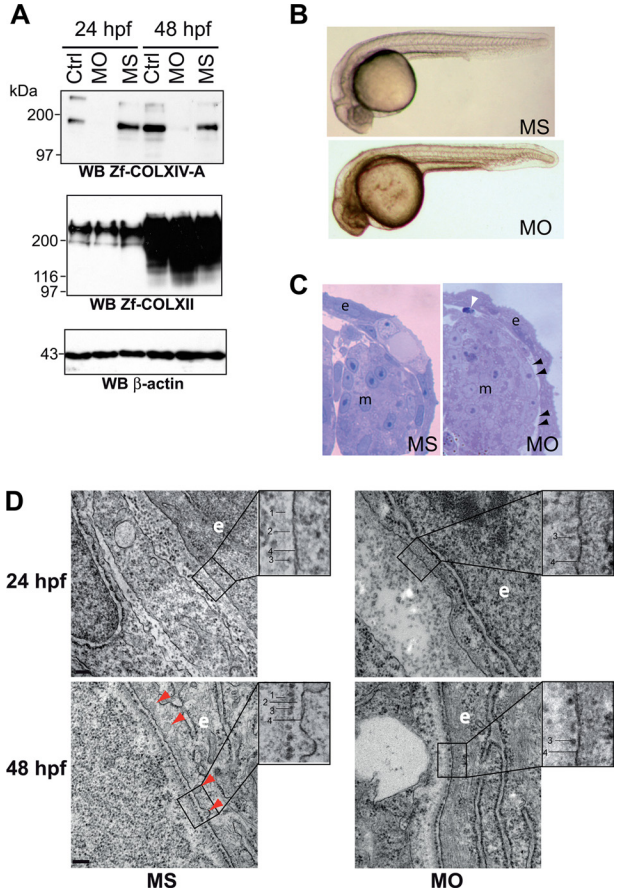

FIGURE 7. **COLXIV-A down-regulation in zebrafish embryos leads to defects in basement membrane formation.** *A*, validation of morpholino-induced COLXIV-A down-regulation. AB/Tu eggs were injected at one cell stage with 4.2 ng of control MS or MO, and collagen expression was analyzed by Western blot. COLXIV-A protein expression was significantly decreased at 24 and 48 hpf in embryos injected with morpholinos against *col14a1a* (MO) as compared with MS-injected embryos whereas COLXII was not affected (n = 3). *B*, knockdown of COLXIV-A expression had no effect on gross morphology of embryos. Injected embryos were analyzed by stereomicroscopy at 24 hpf (n = 5 separate experiments with at least 100 injected embryos/condition in each experiment). *C*, knockdown of COLXIV-A expression caused skin detachment. Transversal thick sections of 24-hpf MO- and MS-injected embryos were stained and analyzed by stereomicroscopy. At this stage, compared with the MS-injected embryos, MO-injected embryos showed zones of epidermal detachment (*e*), resulting in gaps between epidermis and adjacent tissue (*black arrowheads*). In addition, apoptotic cells (*white arrowhead*) were visible beneath the skin. m, muscle. The pictures correspond to the *right upper part* of the embryos at the yolk sac extension level. *D*, knockdown of COLXIV-A expression impairs basement membrane formation. Transmission electron microscope images of MS- and MO-injected embryos at 24 and 48 hpf. At 24 hpf, a basement membrane consisting of electron dense (lamina densa, *line 1*) and electron lucent (lamina lucida, *line 2*) material can be discerned in MS-injected embryos. In addition, sparse adepidermal granules (*line 3*) are visible in the lamina lucida of MS-injected embryos. In contrast, the lamina lucida and lamina densa are missing in MO-injected embryos at 24 hpf, although some adepidermal granules (*line 3*) can be discerned close to the basal plasma membrane (*line 4*). At 48 hpf, adepidermal granules (*line 3*) are homogenously deposited in the lamina lucida (*line 2*) of MS-injected embryos and thus form a nice sheet-like structure. In contrast, in MO-injected embryos, the adepidermal granules are irregularly spaced, showing frequent gaps. Furthermore, the lamina lucida is very thin, and the lamina densa has a fuzzy appearance, indicating defects in BM structure. Moreover, invaginations of the epithelial cell plasma membrane (*line 4*) observed in the MS-injected embryos are less frequent in the morphants (*red arrowheads*). *Scale bars*: 24 hpf, 100 nm; 48 hpf, 200 nm. *WB*, Western blot; *Ctrl*, control.

were thus injected with morpholinos targeted to the translational start site region (MO) or with five-base mismatch control (MS). The specificity and efficiency of MO were checked by

Western blot of total protein extracted from 24- and 48-hpf uninjected (control) and injected embryos (MO and MS) (Fig. 7*A*). The two bands corresponding to the COLXIV-A strongly decreased in lysates of 24 and 48 hpf MO-injected embryos, whereas they were unaffected in MS lysates as compared with uninjected embryos lysates. The gross morphology of MO-injected embryos at 24 and 48 hpf was normal when compared with MS-injected and uninjected embryos (Fig. 7*B*). At the histological level, a detachment of the skin was observed in some areas (Fig. 7*C*, *black arrowheads*). Importantly, this was not simply a fixation artifact, because it was consistently seen in MO-injected but not MS-injected embryos. In contrast, no defects were observed in the epidermis or in other tissues and organs. It has to be noted that the skin detachment was also accompanied by the presence of apoptotic cells in the dermis (Fig. 7*C*, *white arrowhead*). This finding is in agreement with very recent results demonstrating high level of cardiac fibroblast cell death in the postnatal ventricular myocardium of *Col14a1*$^{-/-}$ mouse (31).

To gain a better understanding of the skin detachment phenotype, we next examined the skin with transmission electron microscopy. Transmission electron microscopy revealed that MO-injected embryos had profound defects in the epidermal-dermal BM structure. At 24 hpf, a BM was clearly visible in MS-injected embryos, consisting of electron dense (lamina densa; Fig. 7*D*, *line 1*) and electron lucent (lamina lucida; Fig. 7*D*, *line 2*) zones. In addition, adepidermal granules (Fig. 7*D*, *line 3*) were visible in the lamina lucida. In contrast, MO-injected embryos lacked a lamina lucida and lamina densa at 24 hpf, although some adepidermal granules could be detected close to the plasma membrane (Fig. 7*D*, *line 4*) (Fig. 7*D*, compare *upper right* and *upper left panels*). At 48 hpf, a well delineated lamina densa (Fig. 7*D*, *line 1*) was visible in MS-injected embryos (Fig. 7*D*, *bottom left panel*). In contrast, the lamina densa (Fig. 7*D*, *line 1*) of MO-injected embryos had a fuzzy appearance (Fig. 7*D*, *bottom right panel*). Furthermore, the lamina lucida (Fig. 7*D*, *line 2*) was extremely thin in MO-injected embryos. Also, whereas the adepidermal granules (Fig. 7*D*, *line 3*) were regularly spaced in the MS-injected embryos at 48 hpf, their distribution was uneven in the MO-injected embryos, with frequent gaps (Fig. 7*D*, compare *bottom right* and *bottom left panels*). Interestingly, fewer invaginations of the plasma membrane (Fig. 7*D*, *line 4*) were observed in the MO-injected embryos at 48 hpf (Fig. 7*D*, compare *bottom left* and *bottom right panels*), suggesting that MO-injected embryos may secrete less BM material. Taken together, these results show that the assembly of the BM is severely compromised in MO-injected embryos.

Despite structural defects in the BM, we did not observe a split between the epidermis and the BM. However, we saw frequently ruptures in the dermis (Fig. 7*D*, *upper right panel*). Hence, the detachment of the epidermis appeared to be caused by splits in the dermis. It is possible that tears in the dermis are caused by impaired cohesion of the dermis to the BM. Alternatively, the dysfunctional BM may lead to increased mechanical stress on the dermis, which in turn may cause the dermis to rupture.

DISCUSSION

Collagens XII and XIV May Have Distinct Spatiotemporal Expression Patterns during Zebrafish Development—Collagens XII and XIV are closely related members of a subset of the collagen family, the FACITs (1). Because of their similar structure and overlapping expression pattern, a central question has been whether these two collagens have redundant or distinct functions. Recently, the function of these related FACIT collagens has been in part elucidated by generating null mouse lines for *Col12a1* (32) and *Col14a1* (9) genes, respectively. Whereas COLXIV is involved in the regulation of collagen fibrillogenesis in early development, COLXII displayed a more unexpected function in the control of osteoblast polarity during bone formation. However, possible redundancy of the two collagens has not yet been investigated in collagens XII/XIV null mouse lines. Our data show that collagens XII and XIV may have distinct spatiotemporal expression patterns during zebrafish development. COLXII is expressed throughout development in connective tissues (14), whereas COLXIV-A is transiently expressed in epithelia at 24 hpf. Thus, COLXII appears to localize to connective tissues, and COLXIV-A appears to localize to epithelia.

COLXIV-A Persists in BMs at 48 and 72 hpf—Although COLXIV-A is absent from most epithelia at later time points (48–72 hpf), we could still detect it in BMs, where its expression overlapped with COLXII. BM components are generally made by epithelial cells. However, fibroblasts may synthesize components of the BM zone, the junction between BM and connective tissue. *col14a1a* transcripts were detected in the epidermis, cranial placodes, and endodermal pouches at 24 hpf. However, with few exceptions, COLXIV-A could not be detected in either epithelial cells or fibroblasts at 48–72 hpf. It is therefore unclear which of these cell types is the source of COLXIV-A detected in the BM at these developmental stages. Because collagens are often very stable, it is possible that COLXIV-A incorporated into the BM at 24 hpf persists at 48 and 72 hpf. This is supported by the observation that *col14a1a* transcripts analyzed by RT-PCR are very low from 72 hpf onwards. However, it is also possible that *col14a1a* transcripts are simply below the detection level of ISH at 48 and 72 hpf.

COLXIV-A Is Expressed in Undifferentiated Epithelia—Our data indicate that COLXIV-A is specifically expressed in undifferentiated epithelia. Hence, expression in several epithelia was observed at 24 hpf, but not at 48/72 hpf. Previous work has established that COLXIV is a component of connective tissues. To our knowledge, we are the first to show that COLXIV is a genuine, albeit transient component of epithelia. Basal epithelial cells synthesize components of a provisional ECM during embryogenesis (33), as well as components of the BM. However, in the cranial placodes, COLXIV-A was not only present in basal epithelial cells, but throughout the entire epithelium. Furthermore, in basal epidermal cells, COLXIV-A did not show a polarized distribution; instead, it could be detected at both the apical and basal sides of the cells. This suggests that COLXIV-A synthesized by epithelial cells is not only deposited into the BM but also into the pericellular ECM. Based on its expression pattern, it is tempting to speculate that COLXIV-A plays a role in

the cohesion of epithelia sheets and/or in the outgrowth of epithelial folds, such as the endodermal pouches and the median and apical fin folds. However, in the COLXIV-A knockdown, the cohesion of epithelial sheets was not compromised. Nevertheless, it is possible that epithelial defects did not manifest because of compensation by other ECM proteins.

In other species, COLXIV has not been detected in epithelia, except transiently in basal epidermal or ectodermal cells, suggesting possible differences between species. However, because expression pattern studies of COLXIV in tetrapods have been so far mostly restricted to late developmental stages, this discrepancy may reflect differences between the developmental stages analyzed rather than differences between species. In addition, *col14a1b* may localize to connective tissues, as described for tetrapod COLXIV.

COLXIV-A Is a Component of BMs and Is Needed for BM Assembly—By immunofluorescence, we detected COLXIV-A in several BMs at 24–72 hpf, including the epidermal-dermal BM. Co-staining with laminin and detection of the *col14a1a* transcripts in epithelia at 24 hpf further confirmed that COLXIV-A is a component of embryonic BMs in zebrafish. At 24 hpf, when the epidermis starts to differentiate, the BM is very thin, indicating that BM deposition has just begun (18, 33). At this stage, COLXIV-A is highly expressed in epithelia and can be also detected in the BM. COLXIV-A knockdown impaired the formation of the BM, suggesting that COLXIV-A is needed for the initiation of the BM. Although COLXIV binds to perlecan, a BM proteoglycan, COLXIV binds to neither laminin nor COLIV (34), two scaffold forming BM proteins thought to initialize the assembly of the BM. Also, in contrast to other collagens, COLXIV does not form polymers. How COLXIV-A affects BM initiation is therefore presently unclear. Interestingly, at 48 hpf, BM assembly was still impaired, indicating that other proteins could not fully compensate for the absence of COLXIV-A. It is likely that defects in the BM structure underlie the skin detachment defect observed in the COLXIV-A knockdown. However, in addition, COLXIV-A may also link the BM to the subjacent dermis, and impaired BM-dermis cohesion could contribute to the skin detachment phenotype. Collagen XIV binds to both the BM proteoglycan perlecan and dermal type I collagen fibrils (13, 35), making it an ideal bridging protein. Furthermore, it was recently shown that in humans, COLXIV is present in anchoring plaques, *e.g.*, protein complexes that link the dermis to the BM (13, 35).

Col14a1-null mice do not exhibit skin blistering, and the formation of the epidermal-dermal BM is not obviously affected. However, interestingly, the skin of *Col14a1*-null mice shows decreased resistance to mechanical stress. In agreement with the predicted role of collagen XIV as an inhibitor of lateral fibril growth, *Col14a1*-null mice have thicker collagen fibrils in the tendon, which results in altered mechanical properties of the tendon in pups (*e.g.*, reduced stress resistance). The altered mechanical properties of the skin could therefore also be due to defects in collagen fibrillogenesis. Because COLXIV is also a component of anchoring plaques, subtle defects in dermal-epidermal cohesion may also contribute to the decreased stress resistance of the skin of *Col14a1*-null mice. Our study shows that COLXIV has a role in BM formation, whereas *Col14a1*-null mice were shown to have defects in collagen fibrillogenesis. Clearly, differences between species, *e.g.*, zebrafish and mouse, respectively, could explain these different findings. However, we believe that COLXIV may have different functions in early *versus* late development and that the role of COLXIV in BM formation during embryogenesis may be conserved in tetrapods. In support of this, COLXIV has been detected in the BM of human fetus (5). Defects in BM formation may not become apparent in the *Col14a1*-null mice because of compensation by other ECM proteins or increased redundancy in the ECM of tetrapods.

The fact that COLXIV-A is expressed by undifferentiated but not differentiated epithelia suggests that it could function as signaling molecule that maintains an undifferentiated, proliferative state. At later developmental stages, the balance of BM proteins promoting or inhibiting differentiation could shift toward differentiation. However, no epithelial defects were observed in the COLXIV-A knockdown, suggesting that several ECM proteins may function in providing proliferative cues and inhibiting differentiation during early embryogenesis.

In conclusion, we show that COLXIV-A function is not restricted to the regulation of collagen fibril assembly. Our results revealed a previously unsuspected role of COLXIV-A in undifferentiated epithelia and in BM assembly. We propose that COLXIV may have stage-specific roles in epithelia and connective tissues, respectively.

Acknowledgments—We thank Laure Bernard and Bernard Perret (Plateau de recherche expérimentale et de criblage in vivo (PRECI)) for fish maintenance and Christophe Chamot (Plateau d'Imagerie (PLATIM)) for expert technical assistance with imaging (all from UMS CNRS 3444 Biosciences-Gerland, Lyon, France).

REFERENCES

1. Ricard-Blum, S., and Ruggiero, F. (2005) The collagen superfamily. From the extracellular matrix to the cell membrane. *Pathol. Biol.* **53,** 430–442
2. Castagnola, P., Tavella, S., Gerecke, D. R., Dublet, B., Gordon, M. K., Seyer, J., Cancedda, R., van der Rest, M., and Olsen, B. R. (1992) Tissue-specific expression of type XIV collagen. A member of the FACIT class of collagens. *Eur. J. Cell Biol.* **59,** 340–347
3. Gordon, M. K., Foley, J. W., Lisenmayer, T. F., and Fitch, J. M. (1996) Temporal expression of types XII and XIV collagen mRNA and protein during avian corneal development. *Dev. Dyn.* **206,** 49–58
4. Schuppan, D., Cantaluppi, M. C., Becker, J., Veit, A., Bunte, T., Troyer, D., Schuppan, F., Schmid, M., Ackermann, R., and Hahn, E. G. (1990) Undulin, an extracellular matrix glycoprotein associated with collagen fibrils. *J. Biol. Chem.* **265,** 8823–8832
5. Thierry, L., Geiser, A. S., Hansen, A., Tesche, F., Herken, R., and Miosge, N. (2004) Collagen types XII and XIV are present in basement membrane zones during human embryonic development. *J. Mol. Histol.* **35,** 803–810
6. Wälchli, C., Koch, M., Chiquet, M., Odermatt, B. F., and Trueb, B. (1994) Tissue-specific expression of the fibril-associated collagens XII and XIV. *J. Cell Sci.* **107,** 669–681
7. Keene, D. R., Lunstrum, G. P., Morris, N. P., Stoddard, D. W., and Burgeson, R. E. (1991) Two type XII-like collagens localize to the surface of banded collagen fibrils. *J. Cell Biol.* **113,** 971–978
8. Young, B. B., Gordon, M. K., and Birk, D. E. (2000) Expression of type XIV collagen in developing chicken tendons. Association with assembly and growth of collagen fibrils. *Dev. Dyn.* **217,** 430–439
9. Ansorge, H. L., Meng, X., Zhang, G., Veit, G., Sun, M., Klement, J. F., Beason, D. P., Soslowsky, L. J., Koch, M., and Birk, D. E. (2009) Type XIV

collagen regulates fibrillogenesis. Premature collagen fibril growth and tissue dysfunction in null mice. *J. Biol. Chem.* **284,** 8427–8438
10. Ehnis, T., Dieterich, W., Bauer, M., Lampe, B., and Schuppan, D. (1996) A chondroitin/dermatan sulfate form of CD44 is a receptor for collagen XIV (undulin). *Exp. Cell Res.* **229,** 388–397
11. Imhof, M., and Trueb, B. (2001) Alternative splicing of the first F3 domain from chicken collagen XIV affects cell adhesion and heparin binding. *J. Biol. Chem.* **276,** 9141–9148
12. Klein, G., Kibler, C., Schermutzki, F., Brown, J., Muller, C. A., and Timpl, R. (1998) Cell binding properties of collagen type XIV for human hematopoietic cells. *Matrix Biol.* **16,** 307–317
13. Agarwal, P., Zwolanek, D., Keene, D. R., Schulz, J. N., Blumbach, K., Heinegård, D., Zaucke, F., Paulsson, M., Krieg, T., Koch, M., and Eckes, B. (2012) Collagen XII and XIV, new partners of cartilage oligomeric matrix protein in the skin extracellular matrix suprastructure. *J. Biol. Chem.* **287,** 22549–22559
14. Bader, H. L., Keene, D. R., Charvet, B., Veit, G., Driever, W., Koch, M., and Ruggiero, F. (2009) Zebrafish collagen XII is present in embryonic connective tissue sheaths (fascia) and basement membranes. *Matrix Biol.* **28,** 32–43
15. Westerfield, M. (2007) *The Zebrafish Book*: *A Guide for the Laboratory Use of Zebrafish (Danio rerio)*, 5th Ed., Chapters 1–3, University of Oregon Press, Eugene, OR
16. Kimmel, C. B., Ballard, W. W., Kimmel, S. R., Ullmann, B., and Schilling, T. F. (1995) Stages of embryonic development of the zebrafish. *Dev. Dyn.* **203,** 253–310
17. Hauptmann, G., and Gerster, T. (2000) Multicolor whole-mount *in situ* hybridization. *Methods Mol. Biol.* **137,** 139–148
18. Charvet, B., Malbouyres, M., Pagnon-Minot, A., Ruggiero, F., and Le Guellec, D. (2011) Development of the zebrafish myoseptum with emphasis on the myotendinous junction. *Cell Tissue Res.* **346,** 439–449
19. Bauer, M., Dieterich, W., Ehnis, T., and Schuppan, D. (1997) Complete primary structure of human collagen type XIV (undulin). *Biochim. Biophys. Acta* **1354,** 183–188
20. Schnittger, S., Herbst, H., Schuppan, D., Dannenberg, C., Bauer, M., and Fonatsch, C. (1995) Localization of the undulin gene (UND) to human chromosome band 8q23. *Cytogenet. Cell Genet.* **68,** 233–234
21. Thisse, B., Pflumio, S., Fürthauer, M., Loppin, B., Heyer, V., Degrave, A., Woehl, R., Lux, A., Steffan, T., Charbonnier, X. Q., and Thisse, C. (2001) Expression of the zebrafish genome during embryogenesis (NIH R01 RR15402). ZFIN Direct Data Submission
22. Aubert-Foucher, E., Font, B., Eichenberger, D., Goldschmidt, D., Lethias, C., and van der Rest, M. (1992) Purification and characterization of native type XIV collagen. *J. Biol. Chem.* **267,** 15759–15764
23. Koch, M., Bernasconi, C., and Chiquet, M. (1992) A major oligomeric fibroblast proteoglycan identified as a novel large form of type-XII collagen. *Eur. J. Biochem.* **207,** 847–856
24. Dahm, R., Schonthaler, H. B., Soehn, A. S., van Marle, J., and Vrensen, G. F. (2007) Development and adult morphology of the eye lens in the zebrafish. *Exp. Eye Res.* **85,** 74–89
25. Haddon, C., and Lewis, J. (1996) Early ear development in the embryo of the zebrafish, *Danio rerio*. *J. Comp. Neurol.* **365,** 113–128
26. Hansen, A., and Zeiske, E. (1993) Development of the olfactory organ in the zebrafish, *Brachydanio rerio*. *J. Comp. Neurol.* **333,** 289–300
27. Schlosser, G. (2006) Induction and specification of cranial placodes. *Dev. Biol.* **294,** 303–351
28. Wallace, K. N., Akhter, S., Smith, E. M., Lorent, K., and Pack, M. (2005) Intestinal growth and differentiation in zebrafish. *Mech. Dev.* **122,** 157–173
29. van Eeden, F. J., Granato, M., Schach, U., Brand, M., Furutani-Seiki, M., Haffter, P., Hammerschmidt, M., Heisenberg, C. P., Jiang, Y. J., Kane, D. A., Kelsh, R. N., Mullins, M. C., Odenthal, J., Warga, R. M., and Nüsslein-Volhard, C. (1996) Genetic analysis of fin formation in the zebrafish, *Danio rerio*. *Development* **123,** 255–262
30. Webb, A. E., Sanderford, J., Frank, D., Talbot, W. S., Driever, W., and Kimelman, D. (2007) Laminin alpha5 is essential for the formation of the zebrafish fins. *Dev. Biol.* **311,** 369–382
31. Tao, G., Levay, A. K., Peacock, J. D., Huk, D. J., Both, S. N., Purcell, N. H., Pinto, J. R., Galantowicz, M. L., Koch, M., Lucchesi, P. A., Birk, D. E., and Lincoln, J. (2012) Collagen XIV is important for growth and structural integrity of the myocardium. *J. Mol. Cell Cardiol.* **53,** 626–638
32. Izu, Y., Sun, M., Zwolanek, D., Veit, G., Williams, V., Cha, B., Jepsen, K. J., Koch, M., and Birk, D. E. (2011) Type XII collagen regulates osteoblast polarity and communication during bone formation. *J. Cell Biol.* **193,** 1115–1130
33. Le Guellec, D., Morvan-Dubois, G., and Sire, J. Y. (2004) Skin development in bony fish with particular emphasis on collagen deposition in the dermis of the zebrafish (*Danio rerio*). *Int. J. Dev. Biol.* **48,** 217–231
34. Brown, J. C., Mann, K., Wiedemann, H., and Timpl, R. (1993) Structure and binding properties of collagen type XIV isolated from human placenta. *J. Cell Biol.* **120,** 557–567
35. Maguen, E., Alba, S. A., Burgeson, R. E., Butkowski, R. J., Michael, A. F., Kenney, M. C., Nesburn, A. B., and Ljubimov, A. V. (1997) Alterations of corneal extracellular matrix after multiple refractive procedures. A clinical and immunohistochemical study. *Cornea* **16,** 675–682